

# We are IntechOpen, the world's leading publisher of Open Access books Built by scientists, for scientists

6,900

Open access books available

186,000

International authors and editors

200M

Downloads

Our authors are among the

154

Countries delivered to

TOP 1%

most cited scientists

12.2%

Contributors from top 500 universities



WEB OF SCIENCE™

Selection of our books indexed in the Book Citation Index  
in Web of Science™ Core Collection (BKCI)

Interested in publishing with us?  
Contact [book.department@intechopen.com](mailto:book.department@intechopen.com)

Numbers displayed above are based on latest data collected.  
For more information visit [www.intechopen.com](http://www.intechopen.com)



# Application of J Integral for the Fracture Assessment of Welded Polymeric Components

Zoltan Major, Daniel Kimpfbeck and Matei C. Miron

## Abstract

For many demanding applications of engineering plastics, fracture behaviour under various loading conditions is of prime practical importance. It is well known that fracture properties of plastics are significantly affected by the loading rate, temperature and both local and global stress states. The limitations associated with conventional fracture test methods may, at least in principle, be overcome by the use of appropriate fracture mechanical approaches, which properly account for the temperature and rate dependence of the mechanical behaviour of plastics and should provide geometry-independent fracture toughness values. To provide an additional contribution to this application, fracture tests were performed on both 15- and 20-mm-thick bulk-extruded sheets of a polypropylene random copolymer (PP(RC)) and on four different configurations of their welded joints. The fully ductile fracture range was determined by rate-dependent tests on single CT specimens, and fracture toughness values were derived at the peak loads ( $J_{Fmax}$  and  $CTOD_{Fmax}$ ). Fracture toughness values were determined for stable crack extension based on the  $J-\Delta a$  and/or  $CTOD-\Delta a$   $R$ -curves using single and multiple specimens in terms of various definitions of the crack initiation ( $J_{0.2}$ ,  $J_{0.2BL}$  or  $\delta_{0.2}$ ) toughness values. As expected, both methods revealed distinct differences between the bulk materials and the welded joints. These differences were found to depend on the loading rate, the weld configuration and on the data reduction method ( $J$  integral or  $CTOD$ ).

**Keywords:** bulk polymer, welded polymeric structures, elastic–plastic fracture mechanics (EPFM),  $CTOD$ ,  $J$  integral, ductile-brittle transition

## 1. Introduction

For many demanding applications of engineering plastics, fracture behaviour under various loading conditions is of prime practical importance. In this context it is well known that fracture properties of plastics are significantly affected by the loading rate, temperature and both local (if notches or cracks are present) and global stress states (component geometry or specimen configuration). As a result of the complex effects of these parameters, fracture values determined by conventional test methods (e.g. unnotched and notched Charpy fracture energies) are only of very limited use for material characterisation, especially for engineering design purposes. The limitations associated with conventional testing methods may be overcome by the use of appropriate fracture mechanical approaches, which properly account for temperature and rate dependence of the mechanical behaviour of

plastics and should provide geometry-independent fracture toughness values. However, some basic problems should be addressed [1–9]:

- All fracture mechanic methods and their corresponding fracture toughness values have an applicability limit. This limit is associated with the degree of crack-tip yielding and is attended by both theoretical and experimental consequences. These limits are rate- and temperature-dependent for polymers.
- In general, a brittle-to-ductile transition occurs in the fracture behaviour as the test temperature is increased from low to high temperatures. Due to the viscoelastic nature of plastics, this brittle-to-ductile transition depends on the loading rate and also on the local and global stress state.
- True fracture toughness values should be geometry-independent. Several standards and proposals deal with either simple geometry criteria in terms of specimen thickness and ligament length or with a more complicated definition of the local or global specimen constraints [3, 5, 9]. Finally, the geometry dependence may be investigated using various specimen configurations under bending or tensile loading.
- The concepts and data reduction schemes of various fracture mechanics concepts do not support the continuous characterisation of fracture toughness values over a wide loading rate and temperature range.

### 1.1 Fracture mechanics concepts for various degrees of yielding

In view of the excellent existing literature on various fracture mechanics concepts for different degrees of crack-tip yielding [1–9], no attempt will be made to discuss the subject in great detail. Hence, the following discussion will be restricted to merely referring to the numerous fracture mechanics approaches for monotonic loading.

In a small-scale yielding situation, where linear elastic fracture mechanic (LEFM) concepts may be applied, yielding is limited to a small zone in the immediate vicinity of the crack tip. The relevant crack loading parameters are either the stress intensity factor,  $K$ , or the strain energy release rate,  $G$  [2, 4, 6]. Crack extension usually occurs in an unstable manner, and the relevant fracture parameters for crack initiation are the critical stress intensity factor,  $K_{Ic}$  (also termed fracture toughness), or the critical strain energy release rate,  $G_{Ic}$  (the subscript “ $Ic$ ” stands for mode  $I$  plane-strain conditions). If crack growth occurs in a stable manner,  $K$ - or  $G$ -based crack resistance curves ( $R$ -curves,  $K$  vs.  $\Delta a$  or  $G$  vs.  $\Delta a$  with  $\Delta a$  being the crack extension) are used.

In a larger-scale yielding situation, where elastic–plastic fracture mechanic (EPFM) concepts may be applied, crack-tip yielding is more extensive but does not spread to the lateral boundary of the specimen prior to the onset of crack growth. The relevant crack-tip loading parameters are the crack-tip opening displacement ( $CTOD$ ) [2, 3] and the  $J$  integral [2, 3], respectively. Crack growth occurs either by a small amount of stable crack extension followed by unstable rapid crack growth (semi-ductile) or by stable crack extension without any sign of instability (ductile). The relevant fracture parameters for crack initiation are the critical  $CTOD$  ( $\delta_c$ ) and several definitions of critical  $J$  integral values (onset of stable fracture,  $J_Q$ ,  $J_c$  or plane-strain fracture toughness,  $J_{Ic}$ ), respectively. If crack growth occurs in a stable manner,  $CTOD$  or  $J$ -based crack resistance curves ( $R$ -curves) are used. In the latter case, a value for the tearing modulus may also be derived to characterise crack

propagation. However, there is still a critical debate about geometry independence and hence applicability of these values.

In a cross-sectional yielding situation, where post-yield fracture mechanics (PYFM) concepts are needed, crack-tip yielding is very extensive and spreads to the lateral specimen boundary ahead of the crack prior to crack extension. The relevant crack-tip loading parameters are derived either from the limit load analysis (LLA) [2, 3] or the essential work of fracture (EWF) concept [4]. In this case specimen failure occurs by plastic collapse of the specimen net section. The characteristic fracture parameters for crack initiation are limit load force values, FLL and specific essential work of fracture values,  $w_e$ , respectively. Within the EWF concept, crack extension may additionally be characterised by the specific non-essential work of fracture,  $W_p$ . However, geometry independence is also a critical issue here.

## 1.2 Definition of CTOD

Wells [7, 8] proposed the opening at the crack tip as a measure of the fracture toughness for ductile materials. The critical crack-tip opening displacement (CTOD) was related to the stress intensity factor for small-scale yielding. In case of LEFM, the elastic solution for the CTOD can still be used:

$$CTOD = \frac{4}{\pi} \frac{K_I^2}{E\sigma_{ys}} \quad (1)$$

where  $K_I$  is the stress intensity factor for mode *I* loading, *E* is the elastic modulus and  $\sigma_{ys}$  is the uniaxial yield stress of the specific material (for polymers both are rate- and temperature-dependent).

The direct measurement of CTOD was considered to be difficult until the optical full-field displacement and strain analysis methods were frequently applied. According to the related standard (ASTM E1290), the CTOD is estimated from crack opening displacement (COD) measurements at the specimen surface using a clip-gauge extensometer. The CTOD ( $\delta$ ) can also be separated into two components and calculated from  $\delta = \delta_{el} + \delta_{pl}$ . While the elastic component is equal to Eq. (1), the plastic component,  $\delta_{pl}$ , is obtained from an analysis that assumes a rotation point near the centre of the ligament and can be calculated [9]. The rapid development and frequent use of full-field optical methods for fracture analysis opened new options for the direct CTOD measurements as it is described in [10–12]. The resolution of the entire optical test set-up must be sufficient for determining proper CTOD values [10–12].

## 1.3 *J* integral definition

The theoretical *J* integral concept was proposed by Cherepanov (1967) and Rice (1968) as a path-independent integral and was used originally as a measure of the intensity of elastic-plastic crack-tip fields [13–17]:

$$J = \int_C \left( W dy - T \cdot \frac{\partial u}{\partial x} ds \right) \quad (2)$$

where *W* is the strain energy density, *T* is the traction vector, *u* is displacement vector and  $\partial u / \partial x$  is the deformation gradient. The *J* integral defined by Rice in terms of a line-independent path integral cannot be easily measured experimentally. For

simple bend-type fracture specimens, however, a straightforward analysis has been developed to relate  $J$  to the area under the load versus load point displacement record [9].

For ductile fracture, the toughness can be measured either as a single-point value or as a multi-point function in a resistance curve format and is often characterised by the  $J$  integral [18, 19]. Single-point values are based on selected parts of the load–load-point displacement curves. The energy values are determined up to these selected values, and the  $J$  integral values are calculated based on the simplified definition of the  $J$  integral. In this case, various specimen geometries (SENB and CT) can be tested as single specimen are fractured at a number of different loading rates yielding corresponding fracture parameters for these loading rates. In addition to the plain-sided specimens, in order to reduce the plasticity at the ligament, side-grooves may also be applied (SENB-SG or CT-SG). A data reduction scheme based on numerous values of the  $J$  integral was applied, and corresponding values for  $J$  were determined as follows:

$$J = \frac{\eta(a/W)U}{B(W - a)} \quad (3)$$

where  $U$  is the fracture energy up to the relevant force ( $F_m$  for  $J_m$  or  $J_c$  and  $F_u$  for  $J_u$ ),  $\eta(a/W)$  is a crack length-dependent geometry factor,  $B$  is the specimen thickness (corresponding to  $B_{SG}$ , the net thickness without side-grooves for side-grooved specimen),  $W$  is the specimen width and  $a$  is the crack length. While  $J_c$  is applicable to characterise quasi-brittle failure behaviour (quasi-linear load–displacement behaviour with a sharp load drop at the point of fracture),  $J_m$  and  $J_u$  refer to  $J$  integral definitions in which the peak loads,  $F_m$ , and the ultimate loads,  $F_u$ , respectively, are used in the data reduction procedure for materials with non-linear displacement traces and a certain amount of stable crack extension prior to ultimate specimen failure. Details for the determination of the geometry factor,  $\eta(a/W)$ , are given in [2, 3, 5, 6]. All fracture energy values were corrected by the indentation energy according to a procedure described in [20].

Usually, a  $J$  integral-based resistance curve (i.e. a  $J$ - $R$ -curve) is used to describe a ductile material resistance against stable crack initiation, stable crack growth and tearing instability. In this second case, load–displacement curves can be recorded up to different displacements using several specimens to generate crack extension curves ( $R$ -curves). These specimens will be broken in liquid nitrogen, and the crack length related to stable crack growth is determined on the fracture surface.

These tests can be performed according to proposals by ASTM [9, 18] and ESIS [21] in terms of the values of  $J_{0.2}$ ,  $J_{0.2BL}$ . In the first case,  $J_{0.2}$  values are determined, which characterise the fracture resistance at 0.2 mm of the crack extension. Here, the blunting of the ductile crack-tip deformation is not considered. The consideration of the blunting is rather typical for metals. As the blunting line depends on the yield stress of the material, it will inherently be dependent on the loading rate and temperature for polymers.

For higher testing rates (over 1–10 mm/s depending on the material), a special experimental procedure was developed to determine the  $R$ -curves. In these tests the actuator movement was stopped at various predefined deformations prior to total specimen fracture, and the load and displacement data were recorded. The crack extension-dependent  $J$  integral values were determined according to data reduction procedures described elsewhere [22, 23].

Because of their effectiveness in measuring toughness, the  $J$  integral and  $J$ - $R$ -curve have become the most important material parameters in elastic–plastic

fracture mechanics and have been applied widely in practical engineering. Simultaneously, the *CTOD* values can also be used in *R*-curves. Such fracture toughness values based on the *J*- $\Delta a$  and/or *CTOD*- $\Delta a$  *R*-curves in terms of various definition of the crack initiation ( $J_{0.2}$ ,  $J_{0.2BL}$  or  $\delta_c$ ) may serve as a basis for material characterisation, performance evaluation and quality assurance.

A number of different research groups dealt with various problems of the experimental determination and the application to polymers. It must be highlighted the detailed and comprehensive polymer science-based work of Grellmann and Seidler [22–24] on the field of the determination of structure–property relationships using *J* integral and *CTOD* values for a number of polymeric materials. In addition, this group contributed significantly to the development of the experimental determination of *J* and *CTOD* values at high loading rates. Furthermore, the working group of ESIS TC4 [25–28] provided lot of contributions to the experimental determination of *J* values for polymers.

Elastic–plastic fracture mechanics parameters can also be used for structural damage tolerance assessment, fitness-for-service evaluation, residual strength analysis and structural integrity management for various engineering components and structures, such as pressure vessels and piping in nuclear power plants, onshore and offshore petrochemical vessels and tanks, pipelines in oil and gas industries and aircraft structures [19].

Some fire-service vehicles are equipped with tanks for quenching liquids made from extruded polypropylene copolymer (PP-RC) sheets. Several hundred metres of extrusion welding joints are used in these structures. Due to the geometrical constraints, various weld configurations are used in these tanks. Although, the quality of these welded joints was significantly improved, a large number of different defects and imperfections were recognised in previous experimental investigations. The bulk polymeric material revealed pronounced ductility even at high strain rates and low temperatures. Hence, in addition to the conventional stiffness and strength analysis of the tank, this welded structure was considered as an ideal model component for elastic–plastic fracture mechanics (EPFM) investigations.

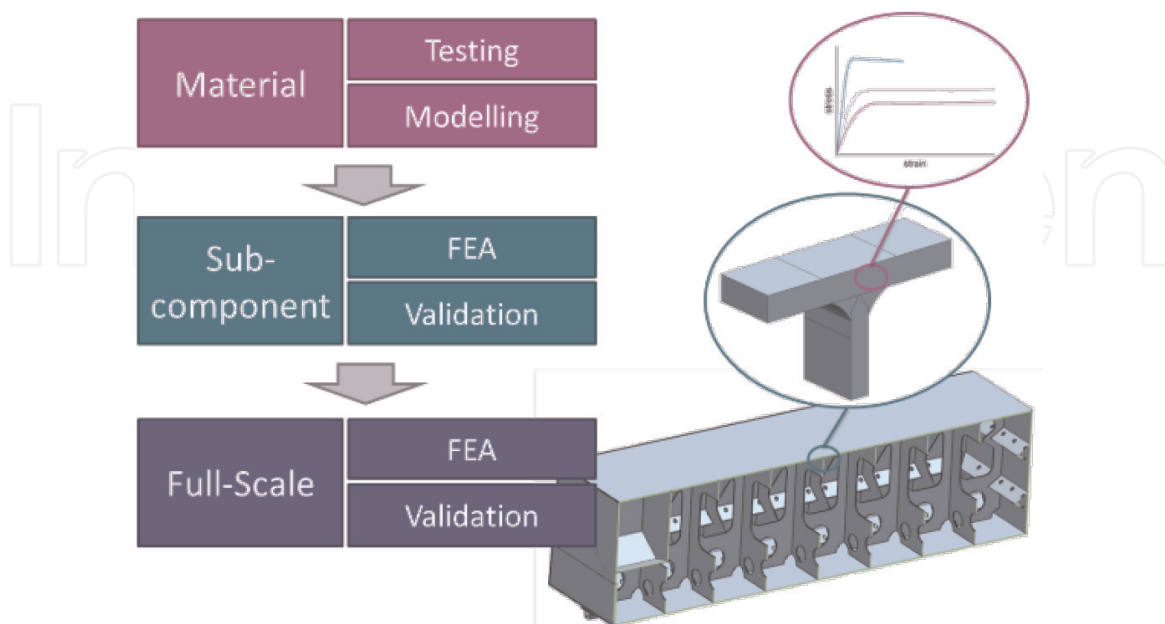


**Figure 1.** Schematic representation of the multi-scale approach for the specific welded polymeric structure. Laboratory specimen level, stress–strain curves (top), welded T-joint (mid) and the entire welded polymeric structure (bottom).

The conventional investigations are summarised in the thesis of Distlbacher [29]. This thesis was structured according to the scale level of analysis, and it is illustrated in **Figure 1**. The complex structure of the tank was broken down into smaller testable subcomponents. The subcomponents represent the various types of join design configurations used in the tank.

## 2. Basic considerations

### 2.1 Experimental techniques of EPFM

#### 2.1.1 Multiple-specimen method of $J$ - $\Delta a$ curve

The different specimens are loaded up to different displacement levels. These displacements generate different lengths of stable crack growth. The  $J$  integral values are calculated using the area of the load–displacement curves up to the corresponding displacement levels. The specimens are then immersed into liquid nitrogen and subsequently broken under impact loading. The stable crack growth is measured on the fracture surface as an average of the crack front from the side to the mid of the specimens. The conventionally calculated  $J$  integral values (energy and geometry factor) can be corrected for large cracks using the  $\Delta a$  values measured. The schematic explanation of the multi-specimen method for determining  $J$ - $R$ -curves is shown in **Figures 2** and **3**:

$$J = \frac{\eta_{el} U_{el}}{B(W-a)} + \frac{\eta_{pl} U_{pl}}{B(W-a)} \left\{ 1 - \frac{(0.75\eta_{el} - 1)\Delta a}{W-a} \right\} \quad (4)$$

The determination of crack resistance curves using multiple specimens is time-consuming and laborious, at least 8–10 specimens should be loaded up to different load levels (displacements). For a statistical evaluation, even more specimens are needed. Hence, there are several efforts to determine reliable  $J$ - $\Delta a$  curves using only a single specimen. For polymeric materials, the detection of the stable crack growth is not always an easy task and the specimen preparation as well as the microscopy could be extremely time-consuming. However, this method allows for the reliable determination of critical  $J$  values with and without blunting line.

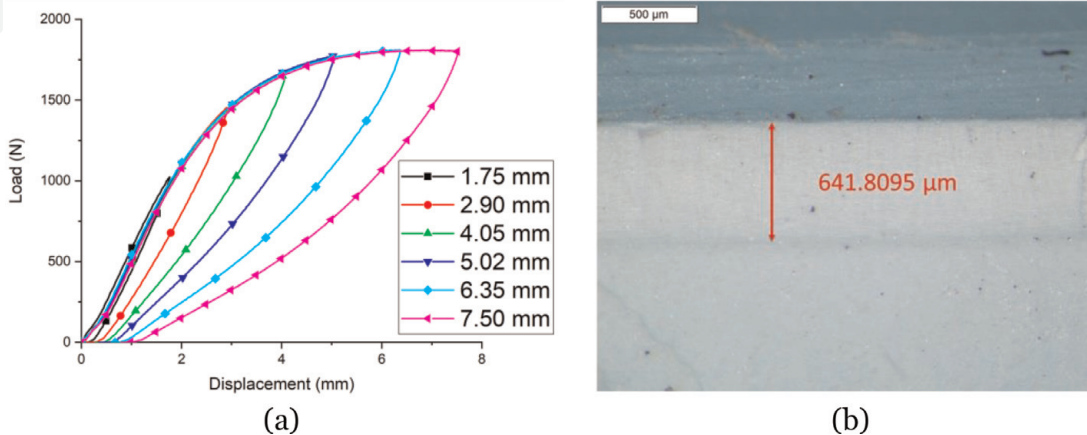


**Figure 2.** Schematic explanation of the multi-specimen method for determining  $J$ - $R$ -curves, (a) load–displacement curves at different displacement levels for the determination of first the energy ( $U_1$  (1.75 mm) to  $U_{max}$  (7.5 mm)) and then the  $J$  integral values, (b) fracture surface with razor blade notch and stable crack growth ( $a_i = 0.642$  mm).

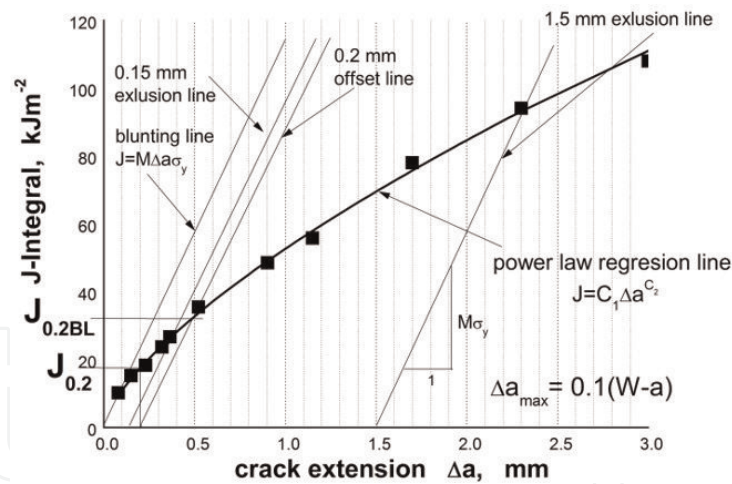


**Figure 3.** Construction of the R-curve,  $J$ - $\Delta a$  values measured and exponential fit curve (R-curve); definition of blunting line and the corresponding  $J_{0.2BL}$  value and definition of  $J_{0.2}$  value. (remark: For polymeric materials the blunting line is loading rate- and temperature-dependent, that is, a unique blunting line belongs to every specific R-curve).

### 2.1.2 Single-specimen methods of $J$ and $J$ - $\Delta a$ curve

- Single parameter
  - Derivation of  $J$  values from the force-displacement curve measured and set  $J_c$  values at a critical force ( $F_{max}$ ).
- Single specimen with load separation principle
  - Sharobeam and Landes presented an experimental procedure based on the load separation principle to construct the material resistance curve of an elastic-plastic material [25, 30].
- Single specimen with semi-cyclic loading
  - Semi-cyclic loading with increasing displacement used. Loading-unloading curves are measured, and compliance method is applied for determining  $\Delta a$  values [9, 19].
- Single specimen with FFSA
  - Novel experimental techniques offer also new options for determining  $J$ - $\Delta a$  curves using a single specimen. Optical full-field deformation measurement (FFSA) with digital image correlation for determining crack-tip opening displacement (CTOD) and crack growth ( $\Delta a$ ) simultaneously was used by several authors recently [10–12] and also in this study.

## 2.2 Application of EPFM methods for polymers

As it was mentioned before, the application of  $J$  integral methods for polymeric materials is focused mainly on material characterisation, quality assurance and on the determination of structure-property relationships. There is hardly any application of fracture mechanics tools for structural integrity management for various engineering components of engineering polymers. The majority of unfilled components are produced as thin-walled injection-moulded components for mass applications. The application of complex fracture mechanics methods for these

components is too expensive, and the risk of such components to fail does not necessitate their application. On the other hand, continuous fibre-reinforced composites reveal predominantly a linear elastic behaviour. Linear elastic fracture mechanics methods both in terms of stress intensity factor  $K$ , but even more frequently in terms of strain energy release rate  $G$ , are widely used for these components. In spite of a high number of investigations, there are still open questions with regard to LEFM; the additional complexity of elastic-plastic method is not rewarded by the users.  $J$  integral values are, however, often calculated in numerical simulations [31, 32] but also predominantly in the linear elastic deformation regime.

It was recognised as an appropriate occasion to apply EPFM methods for large thickness welded polymer structures. These structures were investigated in a contract research project with conventional strength analysis methods for a company partner. Although the majority of these results are confidential, a larger number and high-quality material data were generated:

1. In terms of loading rate- and temperature-dependent true and nominal stress-strain curves on laboratory specimen level
2. Strength analysis of various weld configurations on subcomponent level
3. Stiffness analysis of the entire structure along with the calculation of local stress concentrations

Hence, in addition to the conventional stiffness and strength analysis of the tank, this welded structure was considered as an ideal model component for elastic-plastic fracture mechanics investigations along with some methodological issues.

Based on the above considerations, the main objectives of this paper are:

- To investigate the application of elastic-plastic fracture mechanics methods in terms of  $J$  integral and  $CTOD$  to a bulk (unfilled) polypropylene random copolymer (PP-RC) and its welding joints
- To determine crack resistance curves ( $R$ -curves) along with loading rate-dependent critical fracture toughness values for the bulk polymer and for four configurations of welded joints

### 3. Experimental

The specific material that was used for this fracture mechanics analysis in this study is a Polystone P-RFT® (Röchling Engineering Plastics SE & Co.KG, Haren, Germany) further termed as Polystone PP. Polystone PP is a compound material, with a polypropylene random copolymer (PP(RC)) as a base material. Due to its high strength, high weldability and excellent chemical and corrosive resistance, it is mainly used in chemical engineering and tank building and reveals the following basic properties at room temperature: Young's modulus  $E = 1534$  MPa; Poisson's ratio  $\nu = 0.42$ ; yield stress  $\sigma_y = 30$  MPa; and corresponding yield strain  $\varepsilon_y = 4.0\%$  [29].

Thick extruded neat PP(RC) sheets with a nominal thickness of 15 and 20 mm were provided by the company for these investigations. Compact tension (CT) specimen was manufactured using these plates. The CT specimens were tested under monotonic loading conditions over a loading rate range of 1 to 1000 mm/s.

The geometry of the CT specimens, (a) dimensions, (b) with weld and (c) bulk material, is shown in **Figure 4**.

These extruded Polystyrene PP sheets were welded by extrusion welding using the same material for welding filament at the company partner under controlled conditions. The various weld configurations used here are shown in **Figure 5**. Four different weld seam geometries, square butt welded joint, St; single V butt weld joint, VN-2sp; double V butt weld joint single-sided, 2VN-1sp; and double V butt weld joint double-sided, 2VN-2sp, and two different plate thicknesses 15 and 20 mm were used.

These weld configurations are used in a real welded structure (polymer tank). It must be emphasised here, however, that all four welding configurations have only model character in this study and represent an average of all possible welding quality regarding operator and welding parameters. These welded plates were selected randomly from a larger set of welded plates which were produced for quality assurance purposes. Selected defects in welds are shown in **Figure 6**. These defects range from imperfections (not welded regions) to defects (voids in the weld seam). Polymer welding is frequently used in many practical applications and can be considered as secondary technology for polymer processing. It must be emphasised here, however, that a polymer weld reveals different properties than a usual metal weld. Neither the importance of the welding nor the relative quality compared with the bulk material is at the same level. Our structure represents, even more, an exception for structural design of polymeric structures.

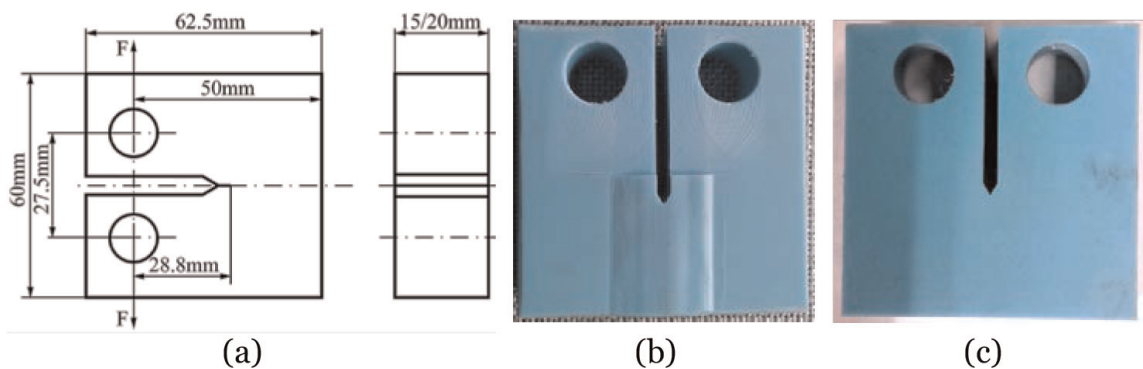


**Figure 4.**  
 Geometry of the CT specimens, (a) dimensions, (b) with weld and (c) bulk material.

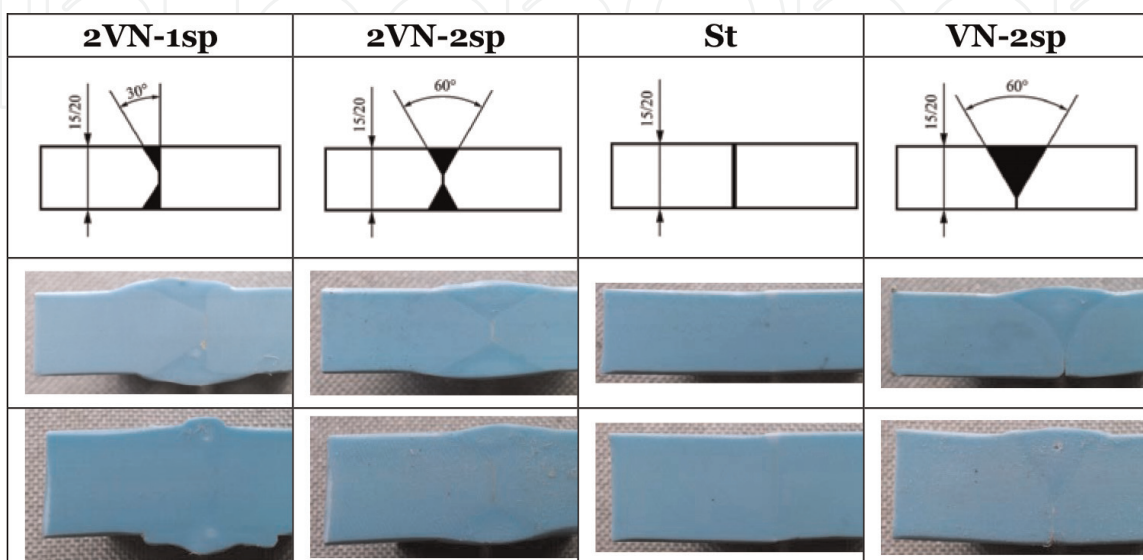


**Figure 5.**  
 The different weld configurations used in this study.

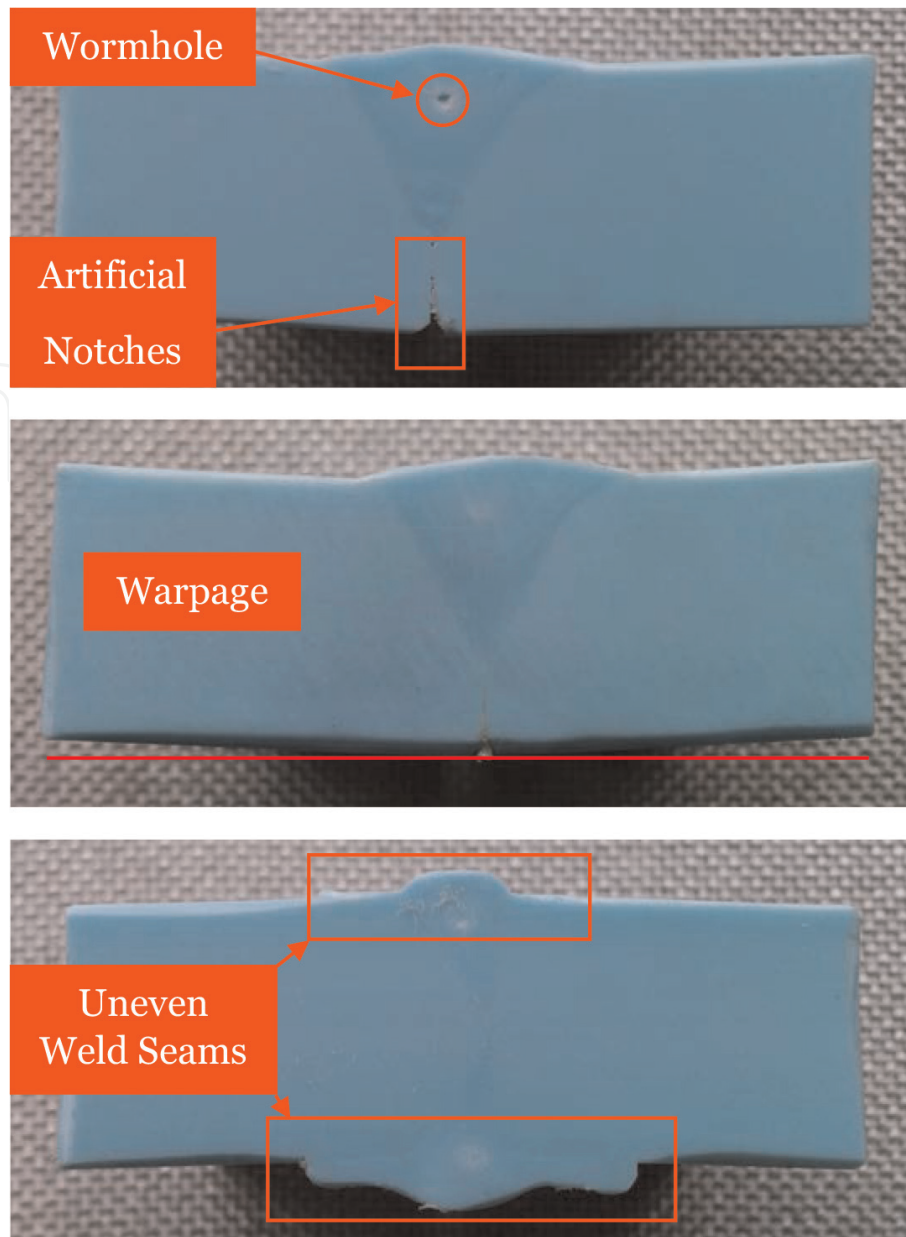


**Figure 6.**  
Detection of various defects in welded polymeric joints.

Schematic representation of the single-specimen method using semi-cyclic loading with increasing displacement along with the fracture surface is shown in **Figure 7**.  $J$  integral values are calculated based on the area below the load–displacement curves for every single loading cycle.

The schematic representation of the optical deformation and strain measurement at the vicinity of the crack tip of the CT specimen are shown in **Figure 8**. A region of interest (ROI) was selected from the entire CT specimen (see **Figure 4**). Local crack-tip deformation ( $CTOD$ ,  $\delta_t$ ) and stable crack growth ( $\Delta a$ ) can be detected simultaneously.

The data reduction scheme of the single-specimen experiments with optical measurements is shown in **Figure 9** (top, force-displacement curves; middle,  $CTOD$ -displacement curves; and bottom, stable crack growth  $\Delta a$ -displacement curves). The determination of fracture toughness in terms of the following parameters was conducted:

- Critical single  $J$  and  $CTOD$  values at the maximum force on the force-displacement curve:  $J_{Fmax}$  and  $CTOD_{Fmax}$

- Critical stable crack initiation values according to the ASTM 1737 proposal using the corresponding blunting lines on the  $J$ - $\Delta a$  curves:  $J_{0.2BL}$
- Determination of  $J_{0.2}$  values at approximately 0.2 mm crack initiation on the combined force-displacement and  $\Delta a$ -displacement curves

The further obvious advantage of this method for practical fracture assessment is the concurrent determination of  $CTOD$  and  $\Delta a$  values. There is a long debate about the selection and applicability of both EPFM methods. While  $CTOD$  is solely a geometrical analysis of the deformation at the vicinity of the crack tip,  $J$  integral allows for a more detailed analysis of the stable crack initiation and crack growth process. It involves the elastic-plastic material model at the vicinity of the crack tip. Ductile fracture is associated with large-scale crack-tip yielding and with extensive

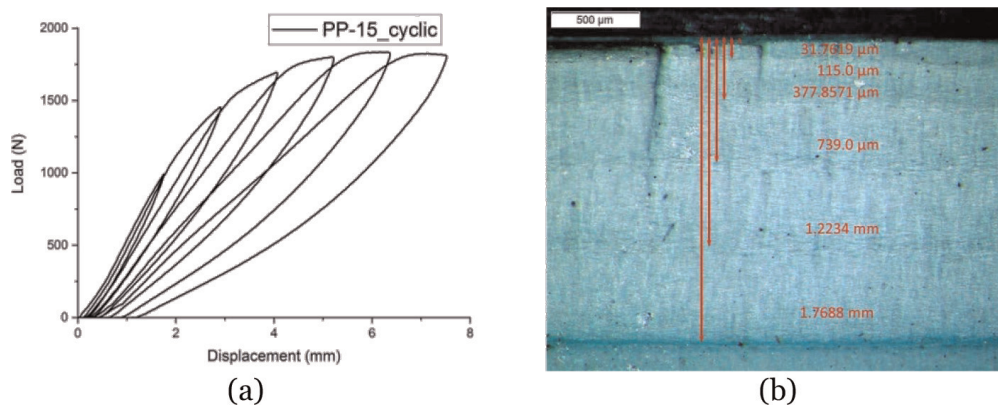


**Figure 7.** Single-specimen method using CT specimen: (a) load-displacement curves of displacement controlled semi-cyclic loading of the specimen for increasing deformations and (b) fracture surface of the CT specimen along with the crack growth marks and the relevant stable crack extension values.

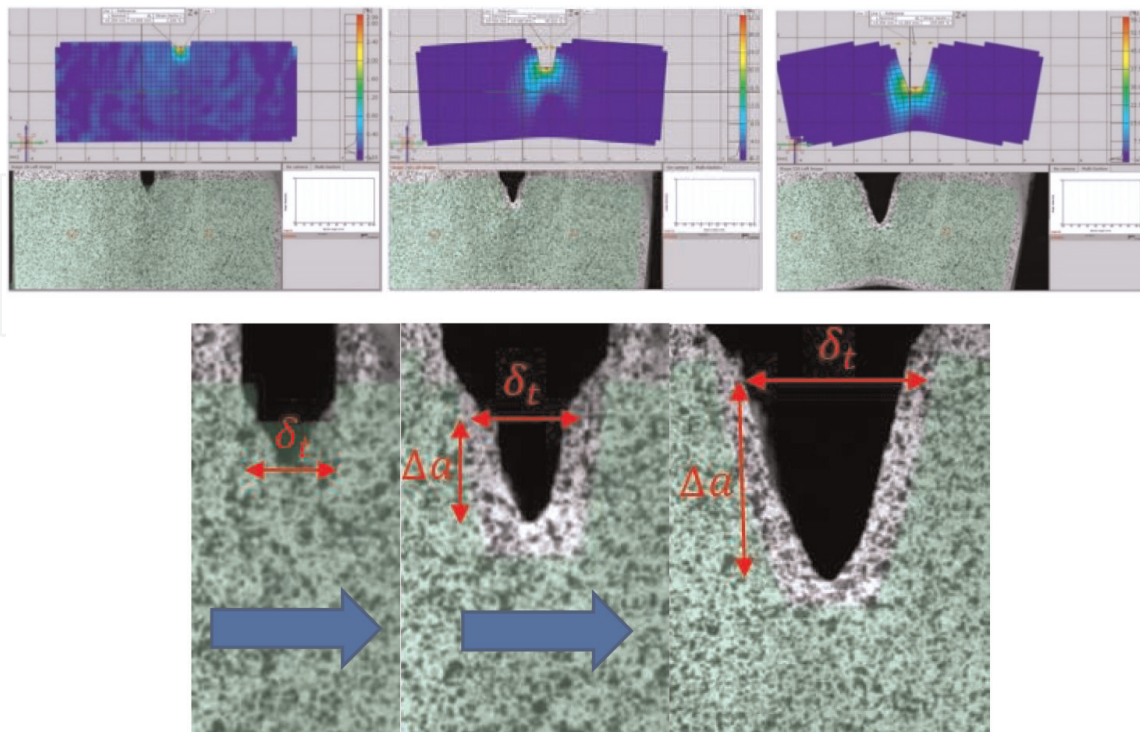


**Figure 8.** Schematic representation of the optical deformation and strain measurement at the vicinity of the crack tip of CT specimens (see **Figure 4**) (top FFSA images). Detection of the crack-tip deformation ( $CTOD$ ,  $\delta_t$ ) and stable crack growth ( $\Delta a$ ) in the ROI (bottom images).

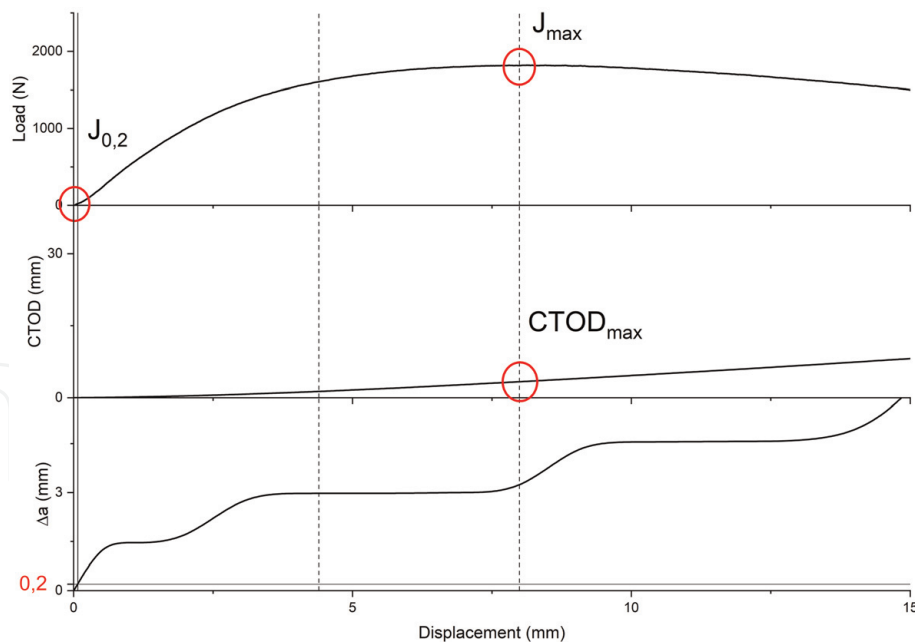


**Figure 9.** Data reduction of the single-specimen experiments with optical measurements: Force-displacement curves (top), CTOD-displacement curves (mid) and stable crack growth  $\Delta a$ -displacement curves (bottom).

crack-tip blunting. The blunting of the crack tip can be characterised by the relationship  $CTOD$  vs.  $\Delta a$ :

$CTOD > 2\Delta a$ , super blunting.

$CTOD = 2\Delta a$ , circular blunting and.

$CTOD < 2\Delta a$ , less blunting, tendency for unstable crack growth.

Furthermore, the kinetic of the crack growth may be characterised by the actual balance between the values of  $CTOD$  and  $\Delta a$ , and based on the actual ratio of these values, the continuity/discontinuity of the crack extension can also be assigned.

The 0.2 mm crack initiation can be considered, however, as an experimentally uncertain limit for the macroscopic image-based single-specimen method. Neither the optical resolution of typical camera systems nor the visibility of the near crack-tip area makes a reliable determination of these values possible. But as neither enough resources were available for the time-consuming multi-specimen method nor a microscope system implemented [22–24] on the test machine was available, the single-specimen method with FFSA was used for the welded joints.

## 4. Results

Single-specimen tests using the load–displacement curves for determining  $J$  values were performed with 20 mm bulk C(T) specimens at loading rates of 1, 10, 100 and 1000 mm/s. The ductile/(semi)-brittle transition was characterised by the appearance of the fracture surfaces along with single  $J_{Fmax}$  values.

Load–displacement curves of 20-mm-thick bulk CT specimens at various loading rates are shown in **Figure 10**. It was speculated previously that the 20-mm-thick specimens reveal a more pronounced ductile-brittle transition and the transition will occur at lower loading rates than for 15-mm-thick specimens. A clear sign of the ductile-semi-brittle transition is visible on both the curves and fracture surfaces. Hence, the ductile regime was selected for further detailed investigations.

Comparison of the  $J$ - $\Delta a$  data points for multiple-specimen method vs. single-specimen methods (monotonic and cyclic) is seen in **Figure 11**. The three  $R$ -curves

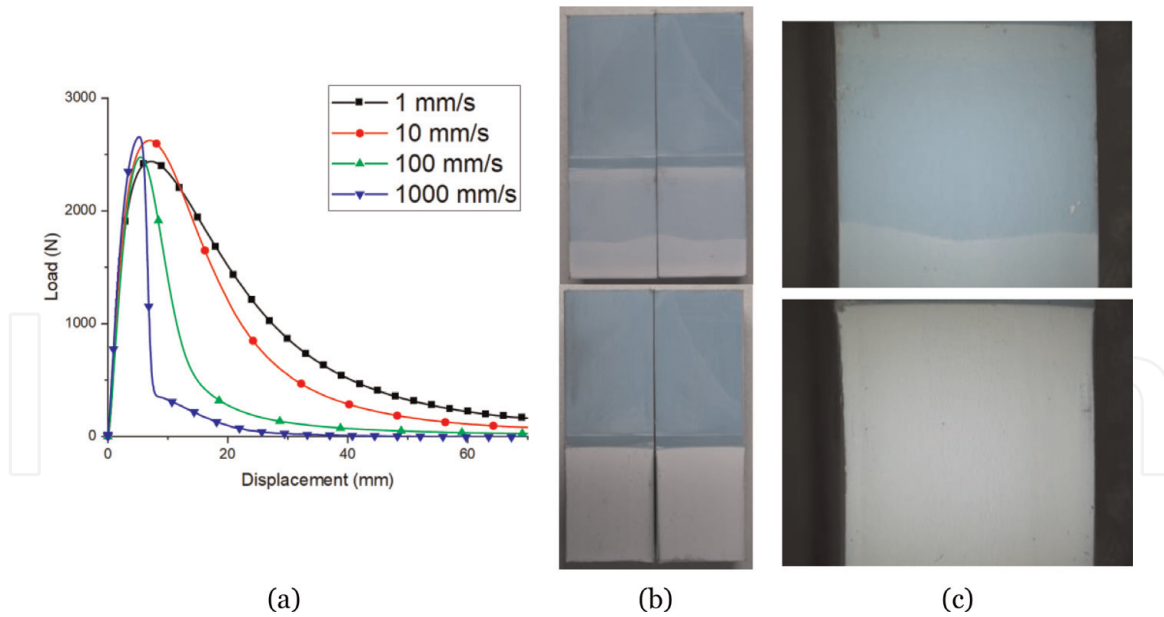


**Figure 10.** (a) Load–displacement curves of 20-mm-thick bulk CT specimens at various loading rates, (b) macro images of tested 20-mm-thick bulk CT specimens at 1 mm/s (bottom) and 1000 mm/s (top) (c) along with fracture surfaces at 1 mm/s (bottom) and 1000 mm/s (top).

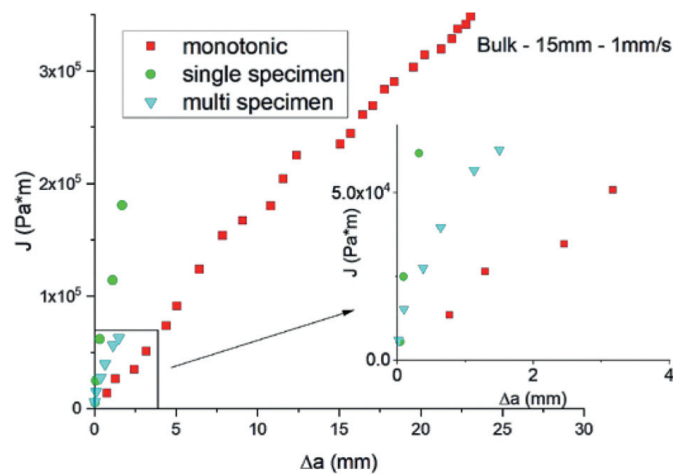


**Figure 11.** Comparison of the J- $\Delta a$  data points for multiple-specimen method vs. single-specimen methods (monotonic and cyclic)—Single-specimen monotonic loading with FFSA (red squares), single-specimen semi-cyclic loading (blue triangles) and multi-specimen (green circles) of a 15-mm-thick PP-bulk specimen obtained at 1 mm/s.

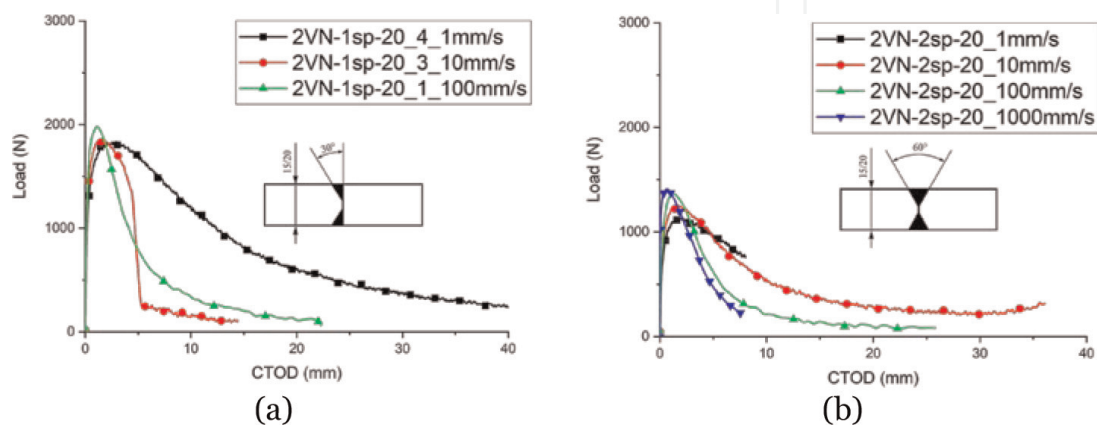


**Figure 12.** Load–CTOD curves of 20-mm-thick welded CT specimens at various loading rates, (a) 2VN-1sp and (b) 2VN-2sp weld configurations.

revealed a sufficient concordance but also clear differences. These differences can be assessed as the experimental evidence of the methods under controlled experimental conditions. We apprehended previously that the optical crack length measurement at the specimen side will not reveal sufficient quality at low crack extension levels. The single-specimen method with FFSA can tendentially be used only for longer crack extension. Nevertheless, for a fast screening, it is a convenient and stable method and exhibits a most conservative measure of the crack resistance (lowest  $J$  values for given crack length). As the amount of specimen and the

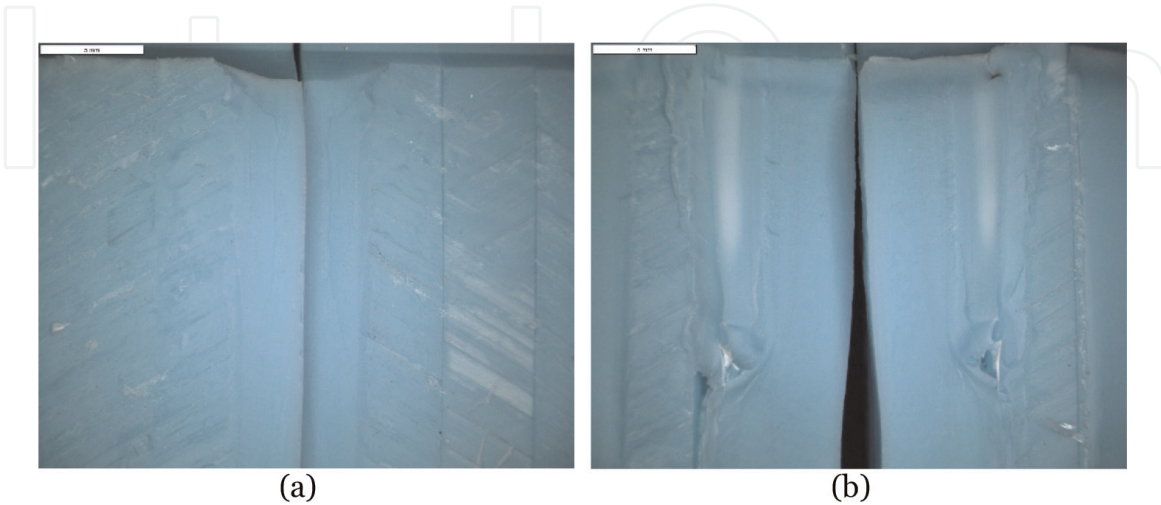


**Figure 13.** Corresponding fracture surfaces at 1 mm/s (a) 2VN-1sp and (b) 2VN-2sp weld configurations. A distinct welding defect is also shown in figure (b).

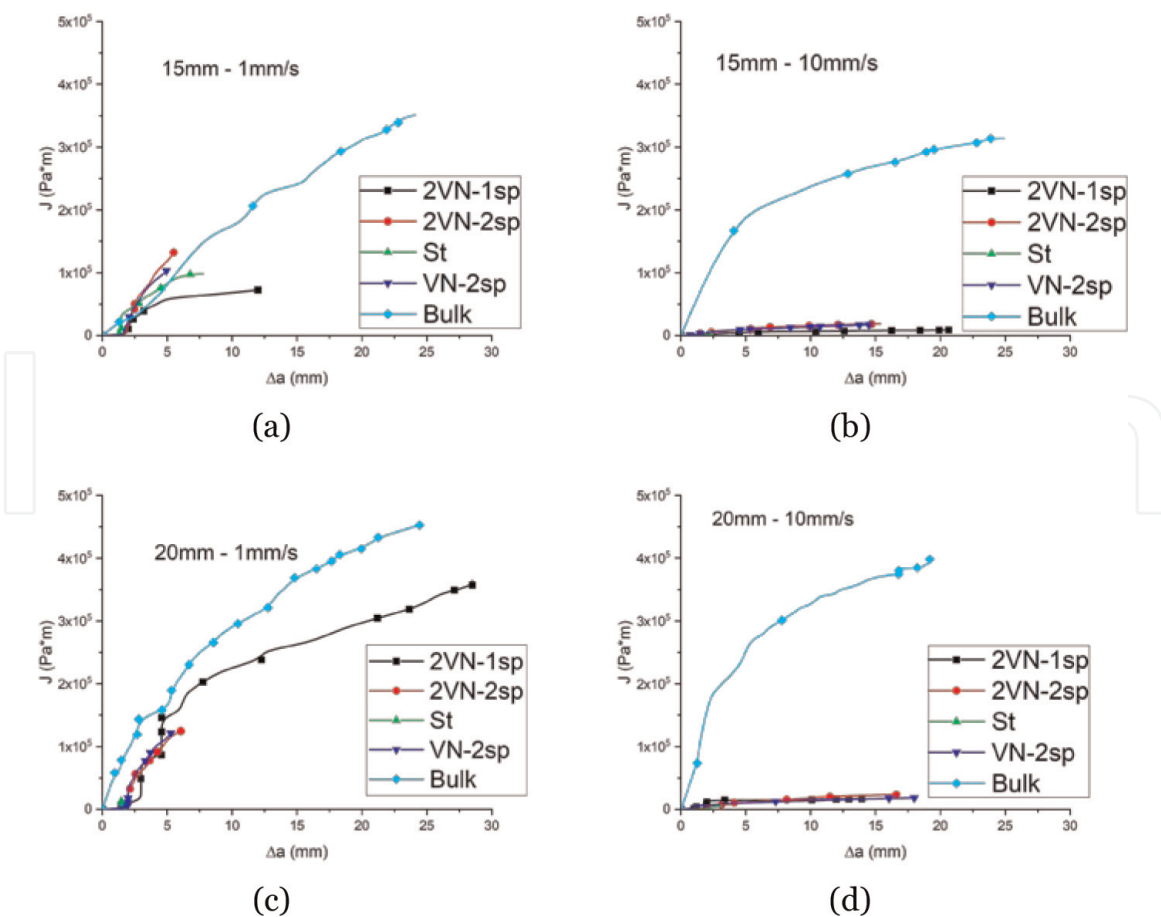


**Figure 14.**  $J$ - $\Delta a$  (R) curves for bulk and for welded material at a loading rate of 1 and 10 mm/s for 15- and 20-mm-thick CT specimens. (a) 1 mm/s, 15 mm thickness, (b) 10 mm/s, 15 mm thickness, (c) 1 mm/s, 20 mm thickness and (d) 10 mm/s, 20 mm thickness.

available laboratory resources were also limited, the welded specimens in the second part of the study have only been analysed by the single-specimen FFSA method.

Single-specimen tests using the load–displacement curves for determining the *J* values were also performed with 15 and 20 mm welded CT specimens at loading rates of 1, 10, 100 and 1000 mm/s. Load–*CTOD* curves of the 20-mm-thick welded CT specimens at various loading rates; (a) 2VN-1sp and (b) 2VN-2sp weld configurations are shown in **Figure 12**. The corresponding fracture surfaces are shown in **Figure 13**. A distinct defect is also seen in the mid of the 2VN-2sp weld.

The load–*CTOD* curves of the welded joints revealed ductile fracture at the testing rate range investigated. While a weak sign of ductile-brittle (semi-brittle) transition was observed above 100 mm/s for 2VN-1sp, all 2VN-sp welded polymeric joints revealed stable tearing.

The fracture surfaces of the broken specimens revealed similar behaviour as the load–*CTOD* curves. In spite of the defects, the two exemplary fracture surfaces reflect ductile fracture at low loading rate. This behaviour was assessed as a kind of damage tolerance at least in the specific loading rate and temperature range.

*J*- $\Delta a$  (*R*) curves for bulk and for welded material at a loading rate of 1 mm/s and 10 mm/s for 15- and 20-mm-thick CT specimens are shown in **Figure 14a–d**.

*CTOD*- $\Delta a$  (*R*) curves for bulk and for welded material at a loading rate of 1 and 10 mm/s for 15- and 20-mm-thick CT specimens are shown in **Figure 15a–d**.

The difference of the *J*-*R*-curves between the bulk and the welded joints was found significantly rate-dependent. While at 1 mm/s, rather a small difference was

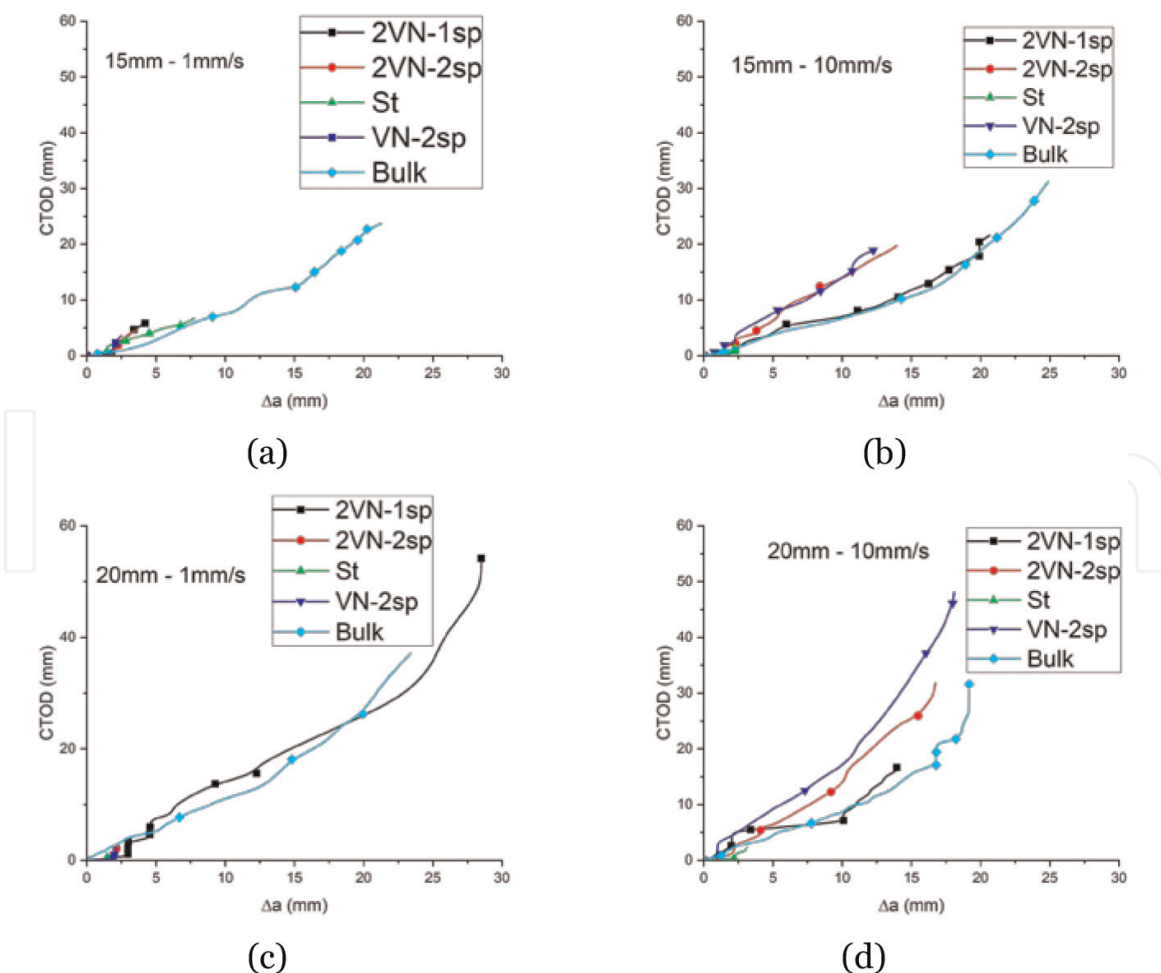


**Figure 15.** *CTOD*- $\Delta a$  (*R*) curves for bulk and for welded material at a loading rate of 1 and 10 mm/s for 15- and 20-mm-thick CT specimens. (a) 1 mm/s, 15 mm thickness, (b) 10 mm/s, 15 mm thickness, (c) 1 mm/s, 20 mm thickness and (d) 10 mm/s, 20 mm thickness.

observed for both thicknesses; a significantly larger difference was obtained for 10 mm/s. The welding joints revealed at 10 mm/s a distinct tendency for an embrittlement. The temporary and local softening of PP(RC) and defects seem to prevent the material from acting ductile and instead enforce brittle behaviour under loading. This tendency can already be observed at loading rates as low as 10 mm/s, whereas the bulk material shows no such behaviour at these loading rates. While the bulk polymer by trend has shown  $CTOD$  values in the range of  $2\Delta a$ , the welded joints revealed values  $CTOD < 2\Delta a$ . Hence, while the bulk has revealed distinct blunting, the welding joints showed less blunting prior to crack growth.

Smaller differences between the bulk and weld were recognised based on the  $CTOD$ - $R$ -curves. In some cases, the welded material revealed similar  $CTOD$  values than the bulk. A possible explanation for these results is that the razor blade pre-crack was positioned in the bulk, either partly or fully (Figure 16).

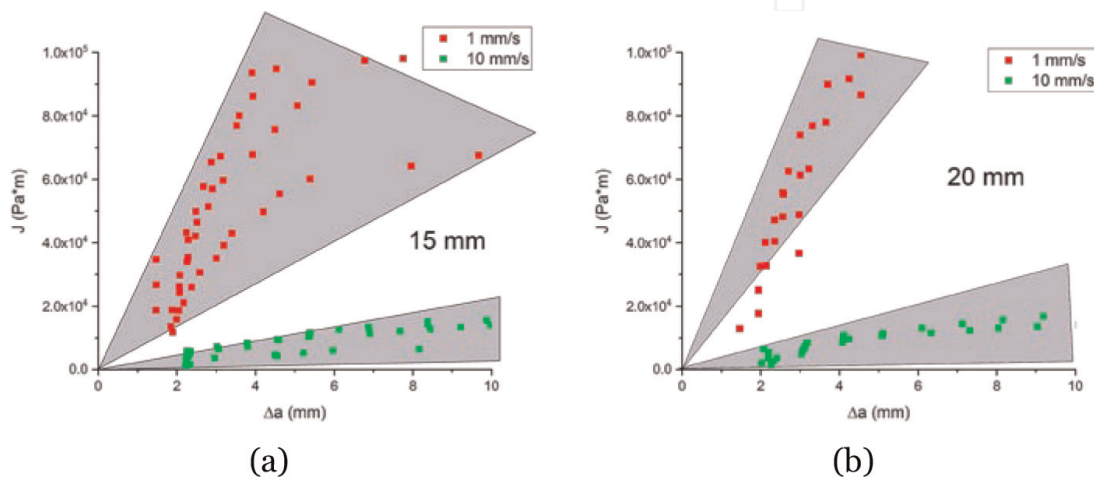


**Figure 16.**

Comparison of the general behaviour tendency for different loading rates for the specimen of all different weldments in terms of  $J$ - $\Delta a$  values for the specimen of (a) 15 mm and (b) 20 mm thickness.

	$J_{Fmax}, \text{kJm}^{-2}$ 15 mm-1 mm/s	$J_{Fmax}, \text{kJm}^{-2}$ 15 mm-10 mm/s	$J_{Fmax}, \text{kJm}^{-2}$ 20 mm-1 mm/s	$J_{Fmax}, \text{kJm}^{-2}$ 20 mm-10 mm/s
2VN-1sp	15	2	75	6.8
2VN-2sp	41	4.1	40	4.2
St	44	2.8	6.6	13
VN-2sp	30	3.2	3.3	40
Bulk	64	62	86	91.9

**Table 1.**

$J_{Fmax}$  values of the bulk PP(RC) and welded joints.

	$CTOD, \text{mm}$ 15 mm-1 mm/s	$CTOD, \text{mm}$ 15 mm-10 mm/s	$CTOD, \text{mm}$ 20 mm-1 mm/s	$CTOD, \text{mm}$ 20 mm-10 mm/s
2VN-1sp	1.4	1.2	3.4	1.8
2VN-2sp	2.3	2.1	2.6	1.9
St	2.3	1.5	2.3	0.5
VN-2sp	2.3	1.9	1.8	2.4
Bulk	2.2	0.6	2.4	1.1

**Table 2.**

$CTOD_{Fmax}$  values of the bulk PP(RC) and welded joints.

The 2VN-1sp weld configurations revealed always high *CTOD* values. Based on the above curves, single fracture toughness values,  $J_c$  in terms of single  $J_{Fmax}$  values,  $J-\Delta a$  curves, as well as  $CTOD_{Fmax}$  values and  $CTOD-\Delta a$  curves were derived. While the determination of the  $J_{Fmax}$  and  $CTOD_{Fmax}$  values was easy and reveal sufficient quality for the material characterisation, the determination of  $J_{0.2}$  values was not possible for the welded joints using the single-specimen FFSA technique. The bulk  $J_{0.2}$  values (2.6–8.2 kJm<sup>-2</sup>) are in a similar range as literature values [20, 22, 30]. The following two **Tables 1** and **2** and contain these values for the four different weld configurations.

## 5. Conclusion

Fracture tests were performed on both 15- and 20-mm-thick bulk-extruded sheets of a polypropylene random copolymer and on their welded joints. After the set of the fully ductile failure regime with regard to the loading rate at room temperature, fracture toughness values were determined both in terms of various single *J* integral and *CTOD* values and in terms of crack resistance ( $J-\Delta a$  and  $CTOD-\Delta a$  *R*-curves). As expected, the polymer investigated revealed a distinct rate dependence over the entire loading rate range investigated. The difference in the fracture behaviour between the bulk and the welded joints was found to be significant in terms of *J* integral-based fracture parameters ( $J_{Fmax}$  and  $J-\Delta a$  curves), and it was also rate-dependent. While at 1 mm/s, rather a small difference was observed; significantly larger difference was obtained at 10 mm/s. Rate-dependent single *F-s* curves for welded joints also support (see **Figure 12a**) this observation. The change of the character of the *F-s* curves in the post-maximum range indicates a smooth ductile to semi-ductile transition. The welded joint reveals constrained deformation around the crack tip.  $CTOD-\Delta a$  curves of the welded joints revealed only slightly higher values than the bulk values at 1 mm/s, and also a smaller stable crack extension was observed. The difference was larger at 10 mm/s; however, the 2VN-1sp weld revealed similar curves than the bulk. The welded polymers can exhibit around the welded joints somewhat lower modulus values (10–15%) [29], that is, at constant displacement larger *CTOD* was expected.

The single-specimen method with FFSA is a suitable fast screening method for characterising the overall fracture behaviour of polymeric test specimens but can practically be used only for longer crack extension. The construction of *J-R* and  $CTOD-R$ -curves was possible for both the bulk and for the welding joints using the single-specimen FFSA method. While the resolution was sufficient for bulk materials also for determining  $J_{0.2}$  values, only  $J_{Fmax}$  and  $CTOD_{Fmax}$  values were determined in sufficient quality for the welded joints of the PP(RC) polymer. The determination of the onset of the stable crack extension and the assignment of  $J_{0.2}$  or  $J_{0.2BL}$  values is uncertain. The obvious advantage of this method for practical fracture assessment is the concurrent determination of *CTOD* and  $\Delta a$  values. The continuity of the stable crack extension can be properly characterised, and the method provides information about the ability for stable tearing of the cracked specimen.

The simplified energy-based calculation scheme for determining fracture toughness values in terms of critical *J* integral values can be applied without any further consideration for material characterisation and for structure–property relationships. The essential use of fracture toughness parameters is in the fracture assessment and dimensioning of components. The usual fracture mechanics-based dimensioning of a component can be described by the simple relationship below:

$$J(a, W, \sigma) \Leftrightarrow J_c(T, d\varepsilon/dt, B) \quad (5)$$

where  $J$  is the non-linear measure of the crack-tip stress intensity (loading) and  $J_c$  is the fracture toughness in EPFM. While  $J$  depends on the crack length, the relevant size of the components and on the remote stress (on the material model, thus indirectly on temperature and loading rate),  $J_c$  depends generally on the loading rate and temperature as well as on the specimen thickness (geometry). While the majority of  $J_{0.2}$  values determined for the bulk were classified as  $J_{Ic}$  values, the other values can only be interpreted as apparent fracture toughness,  $J_c$ . Due to the more strict criteria for fracture instability, the welded joints revealed rather apparent fracture toughness values. Moreover, due to the high data scatter, the EPFM-based fracture assessment of welded PP structures is a challenging task.

The application of fracture toughness values for failure assessment and dimensioning requires a reliable detection of crack-like defects in the component investigated and the determination of proper crack-tip loading parameters for various loading situations and at application temperatures.  $J$  integral values can be calculated for different crack configurations in a structure using finite element methods. These models use the numerical implementation of the original line integral definition of Rice [14, 32]. A proper material model is needed for these simulations, which considers the loading rate and temperature dependence of the elastic-plastic deformation behaviour of the specific polymer [32, 33].

The proper determination of  $J$  integral values for the dimensioning scheme above remains a challenging task to further investigations. As it was described previously, the critical  $J$  integral values can be determined experimentally by:

- Energy-based analysis (force-displacement curves) along with corresponding elastic and plastic geometry factors [9]
- Experimental analysis based on the original Rice  $J$  integral definition using such full-field strain analysis [34, 35]

The applicability to a proper dimensioning necessitates, however, both for the experimental and for the numerical values of the same physical basis and the same mathematical background. This, however, is a highly challenging task, and it requires the determination of experimental  $J$  values based on the original line integral definition of Rice [34]. The determination of fracture toughness and crack-tip loading must follow a consistent scheme and consider the inherent statistical character of both data.

## Acknowledgements

The basic ideas and the first experiments regarding  $J$  integral and CTOD have been performed under the supervision of Prof R. W. Lang in Leoben; I would like to express our very great appreciation to him for his valuable support at that time. Our grateful thanks are also extended to Mrs. Theresa Distlbacher; her master's thesis supported the experiments described in this paper. I would also like to extend my thanks to the technicians, M. Lackner and G. Wurzinger, in my laboratory for supporting the actual experimental work.

IntechOpen

## Author details

Zoltan Major<sup>1\*</sup>, Daniel Kimpfbeck<sup>2,3</sup> and Matei C. Miron<sup>1</sup>

1 Institute of Polymer Product Engineering, Johannes Kepler University Linz, Linz, Austria

2 Institute of Structural Lightweight Design, Johannes Kepler University Linz, Linz, Austria

3 Christian Doppler Laboratory for Structural Strength Control of Lightweight Constructions, Linz, Austria

\*Address all correspondence to: [zoltan.major@jku.at](mailto:zoltan.major@jku.at)

## IntechOpen

---

© 2019 The Author(s). Licensee IntechOpen. This chapter is distributed under the terms of the Creative Commons Attribution License (<http://creativecommons.org/licenses/by/3.0>), which permits unrestricted use, distribution, and reproduction in any medium, provided the original work is properly cited. 

## References

- [1] Blumenauer H, Pusch G. Technische Bruchmechanik. Leipzig Stuttgart: Deutscher Verlag für Grundstoffindustrie; 1993. 3 Auflage. ISBN: 3-342-00659-5; siehe AMK-Büchersammlung unter E 29-3
- [2] Anderson TL. Fracture Mechanics. Fundamentals and Applications. 2nd ed. Boca Raton: CRC Press; 1995. 2. Auflage. ISBN: 978-0849342608; siehe AMK-Büchersammlung unter E 8-1
- [3] Saxena A. Nonlinear Fracture Mechanics for Engineers. Boca Raton: CRC Press; 1997
- [4] Williams JG. Fracture Mechanics of Polymers. In: Ellis Horwood Series in Engineering Science. Chichester: Horwood; 1984
- [5] Kanninen MF, Popelar CH. Advanced Fracture Mechanics. New York: Oxford University Press; 1985
- [6] Broek D. The Practical Use of Fracture Mechanics. Dordrecht: Kluwer Academic Publishers; 1989
- [7] Wells AA. In: Proceedings Crack Propagation Symposium, Cranfield, England; 1961. Vol. 1. Paper B4
- [8] Dugdale DS. Yielding of steel sheets containing slits. Journal of the Mechanics and Physics of Solids. 1960; **8**(2):100-104
- [9] Joyce JA. Manual on Elastic-Plastic Fracture: Laboratory Test Procedures, ASTM Manual Series; MNL 27, ASTM Publication Code Number (PCN): 28-027096-30; 1996
- [10] Xu S, Petri N, Tyson WR. Evaluation of CTOA from load vs. load-line displacement for C(T) specimen. Engineering Fracture Mechanics. 2009; **76**:2126-2134
- [11] Samadian K. Measurement of CTOD along a surface crack by means of digital image correlation. Engineering Fracture Mechanics. 2019;**205**:470-485
- [12] Zhu XK. Comparative study of CTOD-resistance curve test methods for SENT specimens. Engineering Fracture Mechanics. 2017;**172**:17-38
- [13] Cherepanov GP. On crack propagation in continuous media. Applied Mechanics and Mathematics. 1967;**31**:476-488
- [14] Rice JR. A path independent integral and the approximate analysis of strain concentration by notches and cracks. Journal of Applied Mechanics. 1968; **35**(2):379-386
- [15] Hutchinson JW. Singular behaviour at the end of a tensile crack in a hardening material. Journal of the Mechanics and Physics of Solids. 1968; **16**:13-31
- [16] Rice JR, Rosengren GF. Plane strain deformation near a crack tip in a power-law hardening material. Journal of the Mechanics and Physics of Solids. 1968; **16**:1-12
- [17] Begley JA, Landes JD. The J-integral as a fracture criterion. In: National Symposium on Fracture Mechanics; 1971(part II, ASTM STP 514). pp. 1-20
- [18] Zhu XK, Joyce JA. Review of fracture toughness (G, K, J, CTOD, CTOA) testing and standardization. Engineering Fracture Mechanics. 2012; **85**:1-46
- [19] Zhu J. J-integral resistance curve testing and evaluation. Journal of Zhejiang University Science A. 2009; **10**(11):1541-1560
- [20] Major Z. [PhD thesis]. A Fracture Mechanics Approach to Characterize

Rate Dependent Fracture Behavior of Engineering Polymers. University of Leoben; 2002

[21] Blackman B, Pavan A, Williams JG, editors. Fracture of Polymers Composites and Adhesives II, ESIS Publication 32. Kidlington, Oxford, UK: Elsevier; 2003

[22] Grellmann W, Seidler S, editors. Deformation and Fracture Behavior of Polymers. Berlin Heidelberg: Springer-Verlag; 2001

[23] Grellmann W, Che M. Assessment of temperature-dependent fracture behaviour with different fracture mechanics concepts on example of unoriented and cold-rolled polypropylene. *Journal of Applied Polymer Science*. 1997;**66**:1237-1249

[24] Grellmann W, Seidler S. (Hrsg.). *Kunststoffprüfung*. München: Carl Hanser Verlag; 2015. 3. Auflage, S. 258/259. ISBN: 978-3-446-44350-1; siehe AMK-Büchersammlung unter A 18)

[25] Frontini P. On the applicability of the load separation criterion to acrylonitrile/butadiene/styrene terpolymer resins. *Polymer*. 1996;**37**: 4033-4039

[26] Frontini PM. Non-linear fracture mechanics of polymers: Load separation and normalization methods. *Engineering Fracture Mechanics*. 2012; **79**:389-414

[27] Maspoch ML. Fracture characterization of ductile polymers through methods based on load separation. *Polymer Testing*. 2009;**28**: 204-208

[28] Baldi F. Application of the load separation criterion in J-testing of ductile polymers: A round-robin testing exercise. *Polymer Testing*. 2015;**44**: 72-81

[29] Distlbacher T. [MSc Thesis]. Experimental and numerical analysis of large-scale welded polymer structures. Johannes Kepler University; 2014

[30] Gosch A. [MSc thesis]. Examination of J-Integral methods and their applicability to tough polypropylene materials. University of Leoben; 2017

[31] Noels L. Fracture Mechanics, Damage and Fatigue Non Linear Fracture Mechanics: J-Integral, University of Liege, lecture Notes; 2014

[32] Bruyneel M. Computational Fracture Mechanics with SamCef. In: NAFEMS Nordic Regional Conference. Trends and Future Needs in Engineering Simulation. 26–27 October 2010; Gotheburg; 2010

[33] Kimpfbeck D. [BSc Thesis]. Experimental characterisation of fracture mechanical behaviour in welded polymer interfaces. Johannes Kepler University; 2018

[34] Feichter C. [PhD Thesis]. Characterization of the fatigue behavior of elastomer compounds by fracture mechanics methods. University of Leoben; 2006

[35] Kolednik O. A new view on J-integrals in elastic-plastic materials. *International Journal of Fracture*. 2014; **187**:77-107